

1. Optimization results of the different vdW corrections

Table SI. Lattice constants, binding energies and interlayer distances of the Te/BN bilayer with the different configurations as well as the *h*-BN and α -tellurene monolayers

		<i>h</i> -BN	α - tellurene	T ₁ - stacking	T ₂ - stacking	B- stacking	H- stacking
DFT-D2	Latt. (Å)	2.51	4.23	4.33	4.34	4.34	4.34
	E_b (meV)			19	19	19	18
	d_z (Å)			4.03	4.12	4.10	4.01
DFT-D3	Latt. (Å)	2.51	4.22	4.33	4.33	4.33	4.33
	E_b (meV)			-177	-173	-176	-182
	d_z (Å)			3.56	3.61	3.60	3.57
DFT-TS	Latt. (Å)	2.51	4.23	4.34	4.34	4.34	4.34
	E_b (meV)			21	19	18	16
	d_z (Å)			3.98	4.10	4.21	4.06
DFT-dD sC	Latt. (Å)	2.50	4.18	4.33	4.32	4.33	4.33
	E_b (meV)			329	333	330	327
	d_z (Å)			3.61	3.63	3.61	3.60

2. Computational details of the carrier mobilities of α -tellurene and Te/BN bilayer

Using the acoustic phonon limited method, we quantitatively estimate the room-temperature carrier mobility for tellurene and Te/BN bilayer. The carrier

mobility of 2D material is given by $\mu_{2D} = \frac{eh^3 C_{2D}}{k_B T m^* m_d (E_1^i)^2}$, where m^* is the effective

mass in the transport direction and m_d is the average effective mass determined by

$m_d = \sqrt{m_x^* m_y^*}$. The term E_1 represents the deformation potential constant of the

valence-band minimum (VBM) for hole or the conduction-band maximum (CBM) for

electron along the transport direction, defined by $E_1^i = \Delta V_i / (\Delta l / l_0)$. Here, ΔV_i

denotes the energy change of VBM or CBM when tellurene is compressed or dilated

from the equilibrium l_0 by a distance of Δl . The term C_{2D} is the elastic modulus of

the longitudinal strain in the propagation directions (*armchair* or *zigzag*) of the

longitudinal acoustic wave, which can be derived from $(E - E_0) / S_0 = C(\Delta l / l_0)^2 / 2$: E and S_0 denote the total energy and lattice area of tellurene, respectively. We used $\Delta l / l_0$ ranging from -1.0% to 1.0% to fit the values of C_{2D} and E_1^i for α -tellurene and the Te/BN bilayer (Figure S1 and Figure S2), respectively.

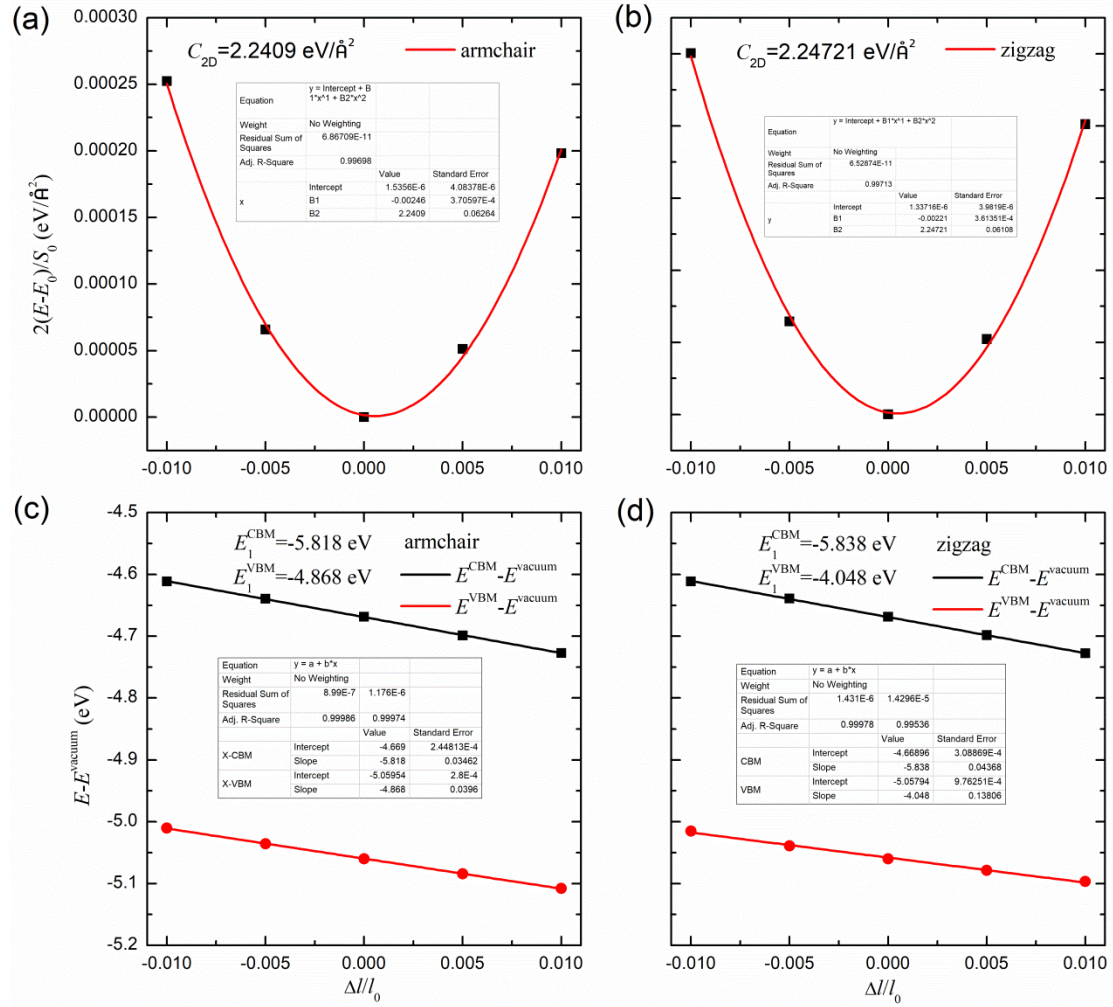


Figure S1. In-plane stiffnesses of deformation potentials of α -tellurene based on PBE+SOC band structures. (a) and (b) are the in-plane stiffnesses in the armchair and zigzag directions, respectively. (c) and (d) are the deformation potentials of the VBM and CBM in the armchair and zigzag directions, respectively.

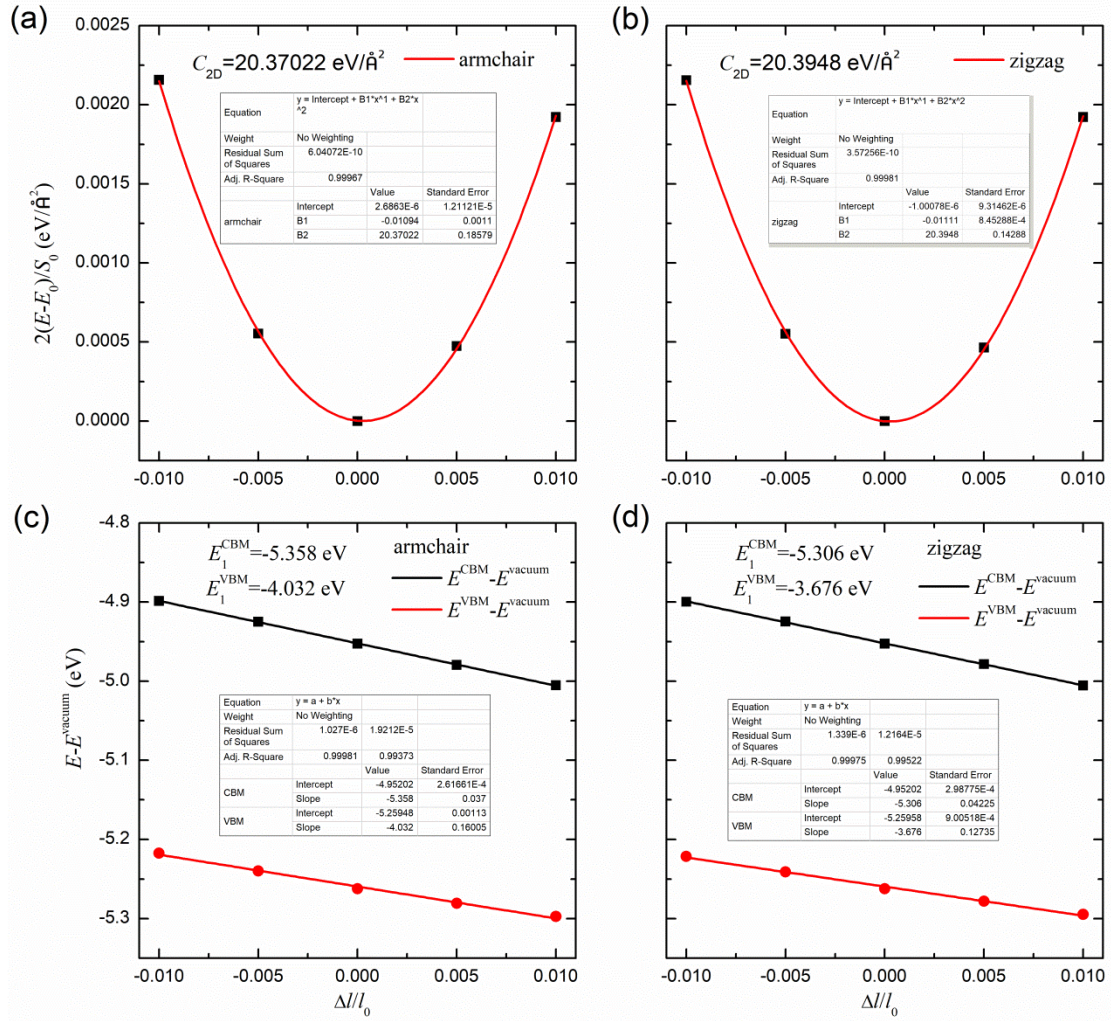


Figure S1. In-plane stiffnesses of deformation potentials of the Te/BN bilayer based on PBE+SOC band structures. (a) and (b) are the in-plane stiffnesses in the armchair and zigzag directions, respectively. (c) and (d) are the deformation potentials of the VBM and CBM in the armchair and zigzag directions, respectively.